
Mercury speciation and exchanges at the air–water interface of a tropical artificial reservoir, French Guiana

B. Muresan^{*1}, D. Cossa^{*}, S. Richard^{**}, B. Burban^{**}

^{*}Institut français de recherche pour l'exploitation durable de la mer (IFREMER), BP 21105, F.44311 Nantes cedex 3, France (EU)

^{**}HYDRECO, Laboratoire de Petit-Saut, BP 823, F.97388 Kourou, French Guiana (EU)

^{*}: Corresponding author : Tel.: 33 6 84 60 54 46; Email: bogdan1977@free.fr

Abstract:

The distribution and speciation of mercury (Hg) in air, rain, and surface waters from the artificial tropical lake of Petit-Saut in French Guiana were investigated during the 2003/04 period. In the air, total gaseous mercury (TGM) at the dam station averaged 12 ± 2 pmol m⁻³ of which > 98% was gaseous elemental mercury (GEM). GEM distribution depicted a day-night cycling with high concentrations (up to 15 pmol m⁻³) at dawn and low concentrations (down to 5 pmol m⁻³) at nightfall. Reactive gaseous mercury (RGM) represented < 1 % of the GEM with a mean concentration of 4 ± 3 fmol m⁻³. Diel RGM variations were negatively related to GEM. In the rain, the sum of all Hg species in the unfiltered (HgTUNF) averaged 16 ± 12 pmol L⁻¹. Temporal distribution of HgTUNF exhibited a pattern of high concentrations during the late dry seasons (up to 57.5 pmol L⁻¹) and low concentrations (down to 2.7 pmol L⁻¹) in the course of the wet seasons. Unfiltered reactive (HgRUNF), dissolved gaseous (DGM) and monomethyl (MMHgUNF) Hg constituted 20, 5 and 5 % of HgTUNF, respectively. All measured Hg species were positively related and displayed negative relationships with the pH of the rain. In the reservoir surface waters, dissolved total mercury (HgTD) averaged 3.4 ± 1.2 pmol L⁻¹ of which 10 % consisted of DGM. DGM showed a trend of high concentrations during the dry seasons (480 ± 270 fmol L⁻¹) and lower (230 ± 130 fmol L⁻¹) in the course of the wet seasons. Diel variations included diurnal photo-induced DGM production (of about 60 fmol L⁻¹ h⁻¹) coupled to minute to hour oxidation / reduction cycles (of > 100 fmol L⁻¹ amplitude). Finally, calculated atmospheric Hg inputs to the Petit-Saut reservoir represented 14 moles yr⁻¹ whereas DGM evasion reached 23 moles yr⁻¹. Apportionment among forms of Hg deposition indicated that up to 75 % of the total Hg invasive flux follows the rainfall pathway.

Keywords: Atmosphere; Artificial reservoir; Mercury; Speciation; Fluxes

1. Introduction

Divalent inorganic mercury (Hg^{II}) in natural surface waters can either be methylated and transferred to the aquatic food webs or, alternatively, be reduced to elemental mercury (Hg^0) and then evolve into the air. Thus, the rate of reduction is of fundamental importance, since this reaction would restrict the quantity of divalent Hg^{II} available for bioaccumulation and auxiliary toxicity in predator animals and human consumers. Because of its high residence time (~ 1 year), Hg is dispersed in the troposphere as gaseous elemental mercury (GEM) (Fitzgerald *et al.*, 1991). However, in the last few years, accumulating evidence has shown that GEM is quickly oxidized as “reactive gaseous mercury” (RGM, presumably composed of HgCl_2) in the atmosphere, leading to a rapid and intensive re-deposition on water surfaces (Lindberg and Stratton, 1998). Thus, to understand the processes and quantify the net exchange, Hg speciation in the atmosphere, as well as speciation in deposition, must be documented. A significant number of studies have provided such data in boreal, temperate and marine environments (e.g., Schroeder *et al.*, 1998; Hedgecock and Pirrone, 2001, Mason and Sheu, 2001 Laurier *et al.*, 2003), while few are available for tropical ecosystems.

The Sinnamary River in French Guiana is 250 km long. Its catchment area spans over 7000 km² of crystalline formation overgrown by uninhabited primary forest. In the 1990s, the Sinnamary River was harnessed by the construction of the Petit-Saut hydroelectric dam *circa* 70 km upstream of the outlet to the Atlantic (Fig. 1). The resulting reservoir lake (5°04' North, 53°03' West) stretches over 60 km in length and width. The maximum water depth reaches 35 m and corresponds to the immersion of 350 km² of uncleared forest (Huynh *et al.*, 1997). According to Richard (1996), the development of such a neotropical water-body has brought about considerable changes in water quality and the natural Hg cycling of the basin of the Sinnamary River.

In the present work, we use the measured Hg concentrations and speciation in air, rain and surface water samples in combination with interfacial transportation models to: (i) examine the atmospheric cycling of Hg in the tropical region of the Sinnamary basin, (ii) describe Hg transformations in the surface waters of the neofomed Petit-Saut reservoir and, (iii) establish a mass balance calculation for Hg exchanges between the reservoir and the surrounding atmosphere. In a general way, the current study aims to demonstrate the role of the Petit-Saut reservoir as a source of elemental Hg for the atmosphere.

2. Material and methods

2.1. Sample collection

2.1.1. Air sampling

In the vicinity of the Petit-Saut dam, temporal distribution and speciation of atmospheric Hg were studied for nearly one year (2003-2004). Excepting the months of September and October 2003, total gaseous Hg (TGM) was uninterruptedly measured from April 2003 to April 2004. The TGM speciation was investigated from January 2004 to April 2004 and for a shorter period between November 2004 and January 2005. It was calculated as the sum of GEM and RGM (Table 1). Additional TGM samplings were made on April 2005 downstream from the outflow of the turbines in the vicinity of an artificial aeration system. Since the turbines are fed with water from the anoxic part of the reservoir, TGM measurements accounted for the partial degassing of discharged hypolimnetic waters during the aeration process.

2.1.2. Rain sampling

Wet deposition was collected at the HYDRECO field laboratory station about 200 m downstream from the dam (Fig. 1). Compiled data account for 20 months of regular sampling from April 2003 to December 2004. Samples for rainfall amount, conductivity, pH and occasionally total organic carbon (TOC) determinations were collected by means of a polyethylene bag. For Hg, the collection system consisted of a 14 cm diameter Teflon (PTFE) funnel attached to a 500 mL acid-clean Teflon (FEP) bottle. A 16 cm long flute of Teflon (PTFE) gently drove the rainfall water directly from the base of the funnel to the bottom of the bottle. Samples were collected on a weekly basis using ultra-clean sampling techniques. The high precipitation (up to 150 mm hr⁻¹) rate allowed rapid collection of the necessary rain amount for analyses and thus limited the Hg photo-reduction and adsorption processes during the rain event (in the range of 5 to 10 minutes). Bottles were double bagged then frozen at -20

°C in dark conditions. Precipitation waters were analyzed for HgT_{UNF} , HgR_{UNF} , DGM and MMHg_{UNF} (see below for definitions).

2.1.3. Surface water sampling

Surface water samples were collected just below the air-water interface (AWI) by immersing an acid clean Teflon (FEP) bottle with a gloved hand (Fig. 1). Analyses of dissolved gaseous mercury (DGM) were performed within 2 hours of collection. The sum of all Hg species (HgT_{UNF}) along with the dissolved (HgT_{D}) and reactive (HgR_{UNF}) fractions were processed the same day. Aliquots were kept to determine monomethylmercury (MMHg) in the unfiltered (MMHg_{UNF}), dissolved (MMHg_{D}) and the particulate (MMHg_{P}) phases. Water samples were filtered using hydrophilic Teflon membranes (0.45 μm pore size, 45 mm diameter, LCR[®], Millipore), then acidified with 0.5 % (v/v) HCl (Suprapur[®], Merck). Used filters (particulate samples) and corresponding filtered solutions were ultimately double bagged and stored at -20 °C in dark conditions until analysis.

2.2. Sample analysis

2.2.1. Ancillary variables

In the epilimnion, measurements for temperature, pH, dissolved oxygen, conductivity and redox were determined *in situ* by means of an YSI multiparameter probe sonde 600XLM. Additional analyses for organic matter (OM) content, pH and conductivity in atmospheric wet deposition were carried out at the HYDRECO field laboratory. Total organic and inorganic carbon in the global and the dissolved fractions were analyzed by IR spectroscopy after oxidative or acidic digestion of the samples.

2.2.2. Atmospheric gaseous mercury

The analyzer systems included an automated Tekran Model 2537A, which was used together with a Model 1130 Speciation Unit to simultaneously monitor GEM and RGM in air. This instrumentation and its implementation are described in detail by Poissant *et al.* (2005). Briefly, the analytical train of the Tekran 2537A instrument is based on the amalgamation of gaseous Hg onto gold cartridges followed by a thermodesorption and analysis by cold vapor atomic fluorescence spectrophotometry. The Model 2537A provided 5-min GEM (part of TGM that passed through the Model 1130) analyses at sub-pmol m^{-3} levels. The analytical precision was estimated to be better than 2 %. During sampling, RGM in the atmosphere was captured in the Model 1130 KCl-coated quartz annular denuder module. The 1130 speciation unit was configured to collect 3 hour samples at a 10 L min^{-1} flow rate. After the 3 hour sampling period, the 1130 Speciation Unit was flushed with Hg-free air, then RGM was thermodesorbed and analyzed. The denuders were biweekly reconditioned using the Tekran protocol (Tekran, 2001).

In 2005, some air measurements were made in the vicinity of the aerators located at the tailrace (the downstream part of a dam where the impounded water re-enters the river) of the turbine where the TGM concentrations were high. We used a portable Hg analyzer RA-915+ (LUMEX) allowing us to get TGM data in a continuous mode with a detection limit of 10 pmol m^{-3} . The RA-915+ Hg analyzer employs the atomic absorption spectrometry technique, which is implemented using the direct Zeeman Effect. No significant differences in the TGM concentrations were observed between both instruments, upon the condition of exceeding the RA-915+ detection limit.

2.2.3. Mercury speciation in water and particles

All Hg species in water samples were detected by cold vapor atomic fluorescence spectrometry (AFS). HgT was determined according to Bloom and Fitzgerald (1988), by the formation of volatile elemental Hg (released by SnCl_2 reduction, after 30 minutes of acidic BrCl oxidation) and its preconcentration on a gold trap. HgR (the easily reducible fraction) was obtained by pH 1 direct reduction with SnCl_2 . Unfiltered samples for DGM (mainly Hg^0) analyses were sparged for 20 min with Hg-free argon at 200 mL min^{-1} . The detection limits, defined as 3.3 times the standard deviation on the blanks, were usually 0.05 pmol L^{-1} for the HgT and HgR, and 25 fmol L^{-1} for DGM. The variation of five replicate samples was lower than 10 %. The accuracy for HgT determinations was regularly checked, using the reference material (ORMS-3) from the National Council of Canada as certified reference material (CRM). MMHg was determined in the unfiltered (MMHg_{UNF}) and dissolved (MMHg_{D}) phases using the method proposed by Bloom (1989) and modified by Liang *et al.* (1994) and Leermarkers *et al.* (2001).

The water samples were stored with 0.5 % (v/v) HCl, which is a reliable method for a 3 week storage period (Parker and Bloom, 2005). MMHg in acidified water was extracted by CH₂Cl₂ and then transferred into 40 mL of Milli-Q water by evaporating the organic solvent. The aqueous solutions were analyzed for MMHg by gas chromatography after ethylation and adsorption / desorption on a Tenax® column. For particulate HgT (HgTP) and MMHgP, an acidic dissolution (with concentrated HCl / HNO₃) of the filtered particles took place before the procedures described previously. Detection limits were 0.01 pmol L⁻¹ and 0.005 pmol g⁻¹ for respectively a 100 mL water and 200 mg solid sample. Precision was below 10 % for all analyses. Using the available reference material (IAEA-405), the accuracy of the method was estimated to be better than 5 % with 91 ± 8 % recovery. The detailed procedure is given by Cossa et al. (2002 and 2003).

3. Tropospheric and surface water characteristics

The Guianese seasonal pattern consists of four uneven periods: the short wet season (from the middle of November to the middle of February), the short summer of March, the long wet season (from April until July) and the long dry season (from the middle of August to the middle of November). The precipitations vary from 1700 mm yr⁻¹ in the Northwest to 3800 mm yr⁻¹ eastward of the Sinnamary basin. The annual recorded rainfall is 3000 mm on average on the shore line from Kourou to Cayenne and reaches 2500 mm on the regions inland. The average intensity of the precipitation is approximately 30-40 mm hr⁻¹ with a duration in the order of 5 to 10 minutes. Crests can exceed 150 mm hr⁻¹ but the duration of such showers is approximately one minute (Meteo-France, weather reports).

Anthropogenic sources of atmospheric compounds are located along the shoreline and constitute the Guianese industry (e.g. the European Space Center), the car emissions and the biomass burning. Natural sources mainly consist of the Atlantic Ocean, the ferrallitic soils and the overlying vegetation (Richard, 2001). In wet seasons, oceanic air masses spread over French Guiana: this source was apparent through sodium, sulfate and magnesium loaded aerosols (up to 50, 8 and 5 nmol m⁻³, respectively). In dry seasons, the intensification of slash-and-burn agriculture induces higher potassium, nitrates and oxalic acid levels (up to 10, 5 and 0.9 nmol m⁻³, respectively). According to Richard (2001), in 1999, the acidity of rainfall significantly correlated with its measured organic acid content. Indeed, between the wet and the dry season of 1999, pH decreased from 5.2 to 4.9 concurrently to a doubling in oxalic and acetic acid concentrations. As a result the anthropic activity may define an important source of volatile organic acids to the local atmosphere including rain and aerosols.

Mean temperatures in the surface waters (0.5 m depth) from the Petit-Saut reservoir and in the atmosphere for the 2003/04 period were 29.7 ± 0.6 and 27.3 ± 0.5 °C, respectively. The pH (6.2 ± 0.2 vs 4.6 ± 0.4 units), conductivity (21.4 ± 0.4 vs 14 ± 8 μS cm⁻¹) and TOC (0.39 ± 0.03 vs 0.10 ± 0.06 mmol L⁻¹) were higher in the surface waters than in rain. In the surface waters, high conductivity (i.e. lowest pH: 5.9 units) depicted the dry seasons whereas low conductivity (i.e. highest pH: 6.5 units) corresponded to the wet seasons. Maxima in redox (Eh) were measured in the dry seasons (340 ± 20 mV) and minima in the wet seasons (290 ± 20 mV). According to Dumestre *et al.* (1999), the dry seasons correspond to high primary production periods and development of phytoplanktonic and phototrophic bacterial communities.

4. Results

4.1. Mercury in air

4.1.1. Gaseous Hg speciation and distribution

During the 2003/04 period, TGM at the HYDRECO laboratory station averaged 12 ± 2 pmol m⁻³. This was similar to the mean North Atlantic level of 11.5 pmol m⁻³ measured by Slerm and Langer (1992). The GEM constituted more than 98 % of TGM. Maxima of GEM concentrations were usually measured in wet seasons (14.5 pmol m⁻³) and minima in the dry seasons (9.8 pmol m⁻³). Typically, GEM displayed a significant (p ≤ 0.05) increase with the percentage of rainfall excess (r² = 0.45; n = 11 and [GEM]_{pmol m⁻³} = 0.03 %Rain_{exce} + 12.3). GEM depicted a regular day-night cycle with high concentrations (up to 15 pmol m⁻³) measured at dawn and low concentrations (down to 5 pmol m⁻³) at nightfall (Fig. 2). RGM represented less than 1 % of GEM with a mean concentration of 4 ± 3 fmol m⁻³. Measured

concentrations varied from the apparatus limit detection (close to 0.05 fmol m^{-3}) up to 180 fmol m^{-3} . The minimum of GEM, usually measured at nightfall, corresponded to a maximum of RGM in the atmosphere (Fig. 2).

The TGM measured downstream from the dam at the tailrace of the turbines ranged from below the detection limit of the LUMEX detector ($\sim 10 \text{ pmol m}^{-3}$) to 115 pmol m^{-3} and averaged $47 \pm 21 \text{ pmol m}^{-3}$. Reaching the artificial aeration system, a vertical profile (from the AWI to 2 m height) of TGM was determined in order to probe the Hg volatilization from dam discharged waters (Fig. 3). Maxima of concentrations were measured at the AWI ($380 \pm 330 \text{ pmol m}^{-3}$) and showed a marked variability (from 95 to 1060 pmol m^{-3}). Higher up, TGM levels underwent a pronounced decrease within the first centimeters: from 380 ± 330 to 120 ± 20 then $33 \pm 2 \text{ pmol m}^{-3}$, respectively, at AWI, 0.5 and 1 m height. TGM concentrations also rapidly diminished with increasing distance from the artificial cascade constituting the aeration system (Fig. 3). At 1 m height, TGM decreased from 23 ± 11 to 13 ± 4 then $< 10 \text{ pmol m}^{-3}$ at 10, 50 and 200 m distance from the aeration system. The low concentrations ($< 10 \text{ pmol m}^{-3}$) indicated that, at these locations and time of year, the plume gas evolved from the aerators was mostly diluted in the atmosphere.

4.1.2. Mercury in the aerosols

HgT_P and MMHg_P were measured in the atmospheric aerosols collected on $0.2 \mu\text{m}$ Teflon filters from the Tekran 2537A analyzer. HgT_P concentrations were 11800 and 4100 pmol g^{-1} (i.e. 0.046 and $0.012 \text{ pmol m}^{-3}$) with respect to the short dry (April 2003) and long wet (June 2004) seasons. MMHg_P concentrations (and methylated percentages) were 310 (2.6 %) and 10 (0.3 %) pmol g^{-1} , respectively.

4.2. Mercury in rain

The monitoring of HgT_{UNF} (Fig. 4) displayed a pattern of high concentrations in the late dry season (up to 57.5 pmol L^{-1} , November 2004) and lower in the wet season (down to 2.7 pmol L^{-1} , March 2004). In the wet season, HgT_{UNF} concentration in rain (84 rain events) averaged $16 \pm 12 \text{ pmol L}^{-1}$ (Table 2). This was within the range of concentrations ($17.8 \pm 2.9 \text{ pmol L}^{-1}$) of the South and equatorial Atlantic environments measured by Lamborg *et al.* (1999). HgR_{UNF} constituted approximately 20 % of HgT_{UNF} . With concentrations varying from 0.1 to 20.8 pmol L^{-1} , its temporal distribution revealed a positive correlation with that of HgT_{UNF} ($r^2 = 0.54$). The high temperature ($H = 466 \text{ atm mol}^{-1}$ at $28 \text{ }^\circ\text{C}$) resulted in low DGM concentrations in rain ($800 \pm 900 \text{ fmol L}^{-1}$). DGM constituted 25 % of HgR_{UNF} (i.e. 5 % of HgT_{UNF}) and displayed an analogous temporal distribution to HgR_{UNF} ($r^2 = 0.73$) and therefore HgT ($r^2 = 0.42$). Regarding MMHg_{UNF} , concentrations varied from 0.05 to 10.2 pmol L^{-1} with a mean value of 0.8 pmol L^{-1} . This was in the high range of values found in the literature ($0.2\text{-}0.8 \text{ pmol L}^{-1}$; Bloom and Watras, 1989; Mason *et al.*, 1997; Lawson and Mason, 2001; Hall *et al.*, 2005). Despite its variability, MMHg_{UNF} showed significant positive correlations with HgT_{UNF} ($r^2 = 0.39$), HgR_{UNF} ($r^2 = 0.52$) and DGM ($r^2 = 0.59$). MMHg_{UNF} concentrations also increased with acidity in rain ($r^2 = 0.52$).

4.3. Mercury in surface waters

4.3.1. In situ Hg speciation

HgT_{UNF} in the uppermost 0.5 m of the reservoir averaged $4.5 \pm 1.8 \text{ pmol L}^{-1}$ of which 75 % ($3.4 \pm 1.2 \text{ pmol L}^{-1}$) was dissolved. The particulate phase represented $1.1 \pm 0.9 \text{ pmol L}^{-1}$ (i.e. $7 \pm 6 \text{ mg L}^{-1}$ of SPM at $230 \pm 190 \text{ pmol g}^{-1}$ of HgT_P). Maxima of HgT_{UNF} (up to 5.5 pmol L^{-1}) were measured during the runoff periods of the short wet seasons. Stations from the ancient Sinnamary riverbed had the highest HgT concentrations: 5.2 ± 1.7 , 3.8 ± 1.0 and 1.4 ± 0.9 (i.e. $270 \pm 230 \text{ pmol g}^{-1}$) pmol L^{-1} , respectively, for HgT_{UNF} , HgT_D and HgT_P . MMHg_{UNF} at the AWI occupied 15 % ($0.6 \pm 0.3 \text{ pmol L}^{-1}$) of the HgT_{UNF} and respectively reached 0.3 ± 0.1 and 0.3 ± 0.2 (i.e. $130 \pm 80 \text{ pmol g}^{-1}$) pmol L^{-1} in the dissolved and particulate phases. Unlike HgT , maxima of MMHg_{UNF} concentrations occurred during the high productivity period of the dry season (up to $0.9 \pm 0.2 \text{ pmol L}^{-1}$). MMHg_{UNF} positively correlated with MMHg_P ($r^2 = 0.84$; $[\text{MMHg}_{\text{UNF}}]_{\text{pmol L}^{-1}} = 0.8 [\text{MMHg}_P]_{\text{pmol L}^{-1}} + 0.3$) but negatively with MMHg_D ($r^2 = 0.55$; $[\text{MMHg}_{\text{UNF}}]_{\text{pmol L}^{-1}} = -3.7 [\text{MMHg}_D]_{\text{pmol L}^{-1}} + 1.7$). The surface water loading with authigenic MMHg was supported by paired distributions of MMHg_P and particulate organic carbon ($r^2 = 0.46$; $[\text{MMHg}_P]_{\text{pmol L}^{-1}} = 5 [\text{POC}]_{\text{mmol L}^{-1}} + 0.7$). Finally, as for HgT species, high MMHg_{UNF} concentrations were measured at the AWI of the ancient Sinnamary riverbed stations (up to 3.8 pmol L^{-1}).

Since volatile dimethylmercury ($\text{H}_3\text{C-Hg-CH}_3$) dissociates to MMHg in acidic waters, DGM was mostly present as Hg^0 . According to Amouroux *et al.* (1999), about 99 % of DGM consisted of Hg^0 . Considering our data (the 2003/04 period), DGM in surface waters averaged $350 \pm 200 \text{ fmol L}^{-1}$ ($n = 70$), which was twice the 1999 measured concentrations (close to 190 fmol L^{-1}). In the dry season, DGM at the AWI constituted $10 \pm 7 \%$ of HgT_D and reached up to 25 % at the ancient Sinnamary riverbed stations (Table 2). The high insolation (occasionally above 1 kWh m^{-2}) coupled to the reduced cloud / vegetation cover depicted the ancient Sinnamary riverbed as a privileged site for DGM production. Indeed, DGM rose from 230 ± 130 to $480 \pm 270 \text{ fmol L}^{-1}$ between wet and dry seasons and from 100 ± 20 to $480 \pm 150 \text{ fmol L}^{-1}$ between the remote flooded forest and the ancient Sinnamary riverbed.

4.3.2. In vitro Hg monitoring

The Hg speciation has been examined for (i) DGM in surface water samples regularly collected during a day long period and (ii) DGM production either in the presence of light or in dark conditions (Fig. 5).

(i) DGM concentrations at the AWI were monitored with a 2 hour time lapse (Fig. 5). Concentrations exhibited a steady increase of $60 \text{ fmol L}^{-1} \text{ h}^{-1}$ that started early in the morning and lasted until late afternoon (640 fmol L^{-1}). As dark conditions prevailed, DGM at the AWI declined ($35 \text{ fmol L}^{-1} \text{ h}^{-1}$) and reached its lowest concentration prior to sunrise (70 fmol L^{-1}). This pattern, observed during the dry season, would be extensively altered by changes in atmospheric conditions. Indeed, the cloudy weather and the homogenized epilimnion that depicted the short wet season ensured low DGM concentrations and poor diurnal variability ($180 \pm 45 \text{ fmol L}^{-1}$).

(ii) DGM was monitored in 50-100 mL of surface water samples taken from two simultaneously collected 2 L stock solutions. One was exposed to the direct sunlight whereas the other was kept in dark conditions (Fig. 5). Both solutions were gently agitated (50 RPM). The temperature was stable (around 29°C). Light exposed samples displayed 3 times higher DGM concentrations than unexposed ones (670 ± 100 vs $220 \pm 150 \text{ fmol L}^{-1}$). Despite the marked shift in concentrations, dark and light exposed water samples exhibited analogous patterns: sequential phases of DGM production and consumption. The overall production / consumption kinetics were 430 and $410 \text{ fmol L}^{-1} \text{ h}^{-1}$, respectively.

5. Discussion

5.1. Mercury in the atmosphere

The proximity to the Atlantic Ocean supposes three distinct sources of atmospheric Hg: (i) the marine aerosols enriched in Na^+ , Mg^{2+} and SO_4^{2-} , (ii) the transatlantic terrigenous source due to the transport on a large scale of African aerosols partially enriched in Ca^{2+} and SO_4^{2-} and (iii) the biogenic source resulting from the local vegetation. According to Meteo-France (2005), the marine source dominated in the course of 2003-2004. As a result, average TGM concentration at the dam station ($12 \pm 2 \text{ pmol m}^{-3}$) was comparable to the mean North Atlantic level of 11.5 pmol m^{-3} (Slern and Langer, 1992).

In humid tropical climates, heavy rainfall increases soil Hg mobility (Guedron *et al.*, 2006). Accordingly, weathering and high average insolation ($> 0.20 \text{ kWh m}^{-2}$) accelerates its change from the oxidised state, Hg^{II} , to the reduced gaseous state, Hg^0 , which escapes into the atmosphere. This was supported by an increase in GEM concentrations (up to 14.5 pmol m^{-3}) in response to the wet season heavy rainfall ($r^2 = 0.45$). Increases in GEM emissions from irrigated soils had also been reported for the Nevada (USA) desert by Lindberg *et al.* (1999). The monitoring of atmospheric Hg exhibited a positive correlation between GEM and pH of rainfall ($r^2 = 0.62$). This relationship (Fig. 6) suggested that acid rains might contribute to washout GEM from the atmosphere. Since pH was positively correlated to the amount of rainfall ($r^2 = 0.42$), the maximum GEM removal would take place in dry seasons. This period displayed highest HgT_{UNF} concentrations in rain (up to 57.5 pmol L^{-1} , November 2004). More striking was the daytime reverse correlation between GEM and RGM: the minimum of GEM, observed during the late day period, corresponded to a maximum of RGM (Fig. 2). According to various authors (Iverfeldt and Lindqvist, 1986; Mason *et al.*, 2001; Poissant *et al.*, 2005), the marked increase in the RGM concentrations would be the result of the photochemically induced oxidation of atmospheric Hg^0 . Although the majority of atmospheric Hg was present in elemental form, RGM has much higher wet and dry deposition rates than GEM. It thus might contribute to the deposition of Hg in the reservoir.

The highest concentrations of HgT_{UNF} in rain were measured in the late dry seasons (Table 2). A possible explanation for these elevated values would be the episodic intensification of slash and burn cultures that release Hg from the vegetation and the soil surfaces. According to Richard (2001), the decline of the marine ionic signature in aerosols (Cl^- , Na^+ and Mg^{2+}), observed during the dry seasons, was concomitant with an increase of the fire signature (i.e. K^+ and NO_3^- species). Another reason accounting for the HgT_{UNF} temporal pattern could be rain acidity. We observed that pH in rain presented lower values in the dry seasons (4.4 units) than in the wet seasons (5.0 units). Acidification of rain through increase in organic (oxalic and/or acetic) acids concentrations (Richard, 2001), would enhance GEM oxidation and promote Hg transfer towards the rain droplets (Fig. 6). According to Gårdfeldt and Jonsson (2003a) and Ababneh *et al.* (2006), chlorides and $\text{HO}_2^*/\text{O}_2^{\bullet-}$ radicals (the oxalate photolysis products) in an aerated solution at pH values of ≤ 4 cause Hg^0 oxidation. Conversely, the low concentrations observed in the wet season indicate the existence of a long-term dilution process that had already been described for the Maryland (USA) seashore by Lawson and Mason (2001). Accordingly, heavy rainfall would simultaneously contribute to the partial removal of the Hg-aerosol bounded fraction and to the dilution of Hg^0 in rain. As the local atmosphere progressively becomes depleted of Hg, concentrations in rain would drop even more.

Regarding Hg speciation in rain, the percentage of HgR_{UNF} (20 % of HgT_{UNF}) was high in comparison with data from temperate latitudes or in the absence of direct oceanic influence (Mason *et al.*, 1997). Yet, it was low compared to central oceanic regions: 72 % of HgT in rainfalls collected above the South and Equatorial Atlantic Ocean (Lamborg *et al.*, 1999). Hence, the $\text{HgR}_{\text{UNF}} / \text{HgT}_{\text{UNF}}$ ratios confirm that the air masses around the Petit-Saut reservoir were typical of those of continental areas with a very strong marine influence. The local concentrations of MMHg_{UNF} significantly increased with rain acidity ($r^2 = 0.52$). This suggests that detected MMHg_{UNF} is either the result of the photochemical degradation of ambient dimethylmercury ($\text{H}_3\text{C-Hg-CH}_3$) or the result of the abiotic methylation within the rain droplets. Since dimethylmercury evasion rates were likely to be low (Section 4.3.1.) and because maxima of MMHg_{UNF} concentrations (up to 10 pmol L^{-1}) occurred in the presence of organic acids (released during the annual slash and burn period), we hypothesized that MMHg in the rain droplets was from abiotic methylation. Such mechanisms (including the presence of organic acids) were investigated by Gårdfeldt *et al.* (2003b).

5.2. Mercury exchanges at the Air-Water interface

The annual precipitation rate for the 2003/04 period averaged 3000 mm. Multiplying this value by the measured concentrations in rain, we determined the Hg wet deposition to the reservoir (Table 3). The HgT_{UNF} , HgR_{UNF} , DGM and MMHg_{UNF} wet depositions averaged 46 ± 35 , 9 ± 11 , 2 ± 3 and $3 \pm 5 \text{ nmol m}^{-2} \text{ yr}^{-1}$, respectively. Transposed to the 2003/04 flooded area ($\sim 230 \text{ km}^2$), the annual amounts of deposited HgT_{UNF} , HgR_{UNF} , DGM and MMHg_{UNF} were 11, 2, 0.5 and 0.7 moles (i.e. 2200, 400, 100 and 140 g). Since the rainfall amount diluted the Hg concentrations, the wet deposition fluxes were balanced during the whole year. However, the dry seasons corresponded to reduced rainfalls with high Hg concentrations ($30 \pm 20 \text{ mm week}^{-1}$ of $20 \pm 14 \text{ pmol L}^{-1} \text{ HgT}_{\text{UNF}}$) whereas the wet seasons accumulated high rainfalls with low Hg contents ($70 \pm 50 \text{ mm week}^{-1}$ of $10 \pm 6 \text{ pmol L}^{-1} \text{ HgT}_{\text{UNF}}$). Except for MMHg_{UNF} , reported values were in the low range of data found in the literature (Mason *et al.*, 1997, 1999). Besides, the total atmospheric deposition of Hg has previously been estimated using ^{210}Pb and HgT data in air, rain and atmosphere ("Mercure en Guyane" program, 2001). According to these authors, Hg deposition within the reservoir area reaches a minimum of $60 \text{ nmol m}^{-2} \text{ yr}^{-1}$. Analogous estimates were reported by Lacerda *et al.* (1999) for the whole Amazonian basin ($40\text{-}60 \text{ nmol m}^{-2} \text{ yr}^{-1}$). With $46 \text{ nmol m}^{-2} \text{ yr}^{-1}$, wet deposition corresponded to up to 75 % of total atmospheric Hg deposition. This result underlines the fact that rainfall represents an efficient pathway for atmospheric Hg to reach the Petit-Saut reservoir.

As previously shown by Peretyazhko *et al.* (2006), DGM peaked at the AWI of the reservoir due to photochemical reduction of dissolved Hg species. Both DGM and GEM at the AWI showed a broad variability with insolation that drove photochemical and photosynthetic processes (Figs. 2 and 5). Despite the fact that the maximum production rate was observed during the day period, all water samples were found supersaturated with DGM relative to the atmosphere. As the surface waters represented a potential source of Hg^0 to the atmosphere, the lake-air transfer was estimated by the following relation:

$$\text{Flux} = K (C_a H^{-1} - C_w)$$

where C_a is the air concentration of GEM ($12 \pm 2 \text{ pmol m}^{-3}$) and C_w the water concentration of DGM ($350 \pm 200 \text{ fmol L}^{-1}$). Long-term stability of temperature and wind speed ensured good precision of the various model parameters (Section 3). The mass transfer coefficient of Hg^0 ($K = 3.4 \pm 1.5 \text{ cm h}^{-1}$) was correlated with the mass transfer of CO_2 across the air-water interface (Wanninkhof et al., 1985; Hornbuckle et al., 1994):

$$K = (0.45 U_{10}^{1.64}) [Sc_w(\text{Hg}^0) / Sc_w(\text{CO}_2)]^{-0.5}$$

where U_{10} is the wind speed ($3 \pm 1 \text{ m s}^{-1}$) at 10 m, $Sc_w(\text{CO}_2)$ and $Sc_w(\text{Hg}^0)$ are the Schmidt numbers for Hg^0 and CO_2 in water (560 and 315 at 28°C). The Henry coefficient ($H = 466 \text{ atm mol}^{-1}$ at 28°C) is calculated using the temperature-corrected dependency

$$\text{Log } H = -1078/T + 6.25 ; T \\ (\text{°K}).$$

The Hg^0 effluxes averaged 400 ± 240 and $130 \pm 100 \text{ pmol m}^{-2} \text{ d}^{-1}$ in the dry and wet seasons. On an annual basis, the AWI degassing reached $90 \pm 50 \text{ nmol m}^{-2} \text{ yr}^{-1}$ (Table 3). This was comparable to several temperate lakes from Wisconsin (Vandal et al., 1991), Ontario (Amyot et al., 1997b) or Michigan (Mason and Sullivan, 1997). Comparatively, the Hg^0 efflux from the Petit-Saut reservoir was twice as large as the wet mean deposition of HgT_{UNF} ($46 \pm 35 \text{ nmol m}^{-2} \text{ yr}^{-1}$). Yet, this ratio displayed a broad seasonal variability as wet deposition prevailed during wet seasons (150 vs $130 \text{ pmol m}^{-2} \text{ d}^{-1}$) while effluxes dominated during dry seasons (400 vs $100 \text{ pmol m}^{-2} \text{ d}^{-1}$).

The diel variations of aquatic DGM anticorrelated with atmospheric GEM but were analogous to RGM pattern (see Sections 4.1. and 4.3.). RGM is thought to be produced through photolytic degradation of GEM (via potential reactions with O_3 , H_2O_2 , OH^\cdot , etc.) and also constitutes a privileged sink for gaseous atmospheric Hg towards rain and/or aerosols (Lu and Schroeder, 1998; Hedgecock et al., 2003; Poissant et al., 2005). Thus, RGM production and deposition may determine the Hg atmospheric lifetime. The local RGM deposition was determined through the formula proposed by Laurier (pers com.):

$$\text{Flux} = k_A (\text{RGM})$$

where k_A is the air-side mass transfer coefficient ($1.6 \pm 0.7 \text{ cm s}^{-1}$) calculated using the air-side diffusion coefficient ($D_A = 0.28 \text{ cm}^2 \text{ s}^{-1}$) and the wind speed 10 m above the water surface ($U_{10} = 3 \pm 1 \text{ m s}^{-1}$)

$$k_A = D_A^{0.5} [(0.98 \pm 0.1) U_{10} + (1.26 \pm 0.3)]$$

where \pm is the 95 % confidence interval. The mean RGM deposition was $2.0 \pm 1.5 \text{ nmol m}^{-2} \text{ yr}^{-1}$, which represented 4 and 13 % of the wet and dry HgT deposition, respectively (Table 3). Recorded patterns of DGM, GEM and RGM concentrations (Figs. 2 and 5) suggested that atmospheric gaseous Hg is preferentially oxidized during the day period (maximum of RGM), contributing to the observed decrease of GEM (around 8 pmol m^{-3}) and the increase of DGM (350 pmol m^{-3}). Considering that GEM from the first few 10 m height air-column is readily transferable as RGM to the reservoir, the diel atmospheric deposition would represent close to 20 % of the AWI measured DGM increase. In these particular conditions, the calculated deposition flux should average $150 \pm 100 \text{ pmol m}^{-2} \text{ d}^{-1}$, which is compatible with the total atmospheric deposition ranges but exceeds that of reactive Hg (160 and $5 \text{ pmol m}^{-2} \text{ d}^{-1}$, respectively). This result underlines that either (i) RGM production and subsequent

deposition occurs in the close vicinity (< 1 m distance) of the AWI and/or (ii) that RGM production takes place during short spans (less than a few hours) of intense solar exposure.

5.3. AWI mercury transformations and budget

At the AWI, redox conditions and biologically mediated reactions are expected to play a major role in controlling the availability of Hg species for reduction / oxidation processes (Beucher *et al.*, 2002; Lanzillotta *et al.*, 2004; Peretyazhko *et al.*, 2005). In order to probe these transformations, let us consider the *in situ* and incubation experiments presented in Section 4.3. (Fig. 5). From the *in situ* experiment (i) we concluded that light exposure significantly enhances the overall DGM levels (Amyot *et al.*, 2001). According to Beucher *et al.* (2002), AWI maxima DGM concentrations (10 % of the HgT_D) reflect the photochemical production of Hg⁰ in the presence of a reductive agent such as organic matter and especially iron-carboxylated ionic complexants. Experiment (ii) showed that direct light exposure barely accounted for the observed minute to hour scale variations (on the range of the 0.1 pmol L⁻¹). Rapid Hg oxidation / reduction mechanisms have already been reported in the literature by Siciliano *et al.* (2002) and Garcia *et al.* (2005). Accordingly, observed variability reflected the response of (epi)neuston to the photochemical or endogenous production of oxidant species (O₃, H₂O₂, OH[·], etc.).

As shown in Section 5.2. (and in Fig. 7), the 2003/04 annual Petit-Saut reservoir wet depositions averaged 11, 2, 0.5 and 0.7 moles (i.e. 2200, 400, 100 and 140 grams) for HgT_{UNF}, HgR_{UNF}, DGM and MMHg_{UNF}, respectively. With 46 ± 35 nmol m⁻² yr⁻¹, the HgT_{UNF} wet atmospheric deposition constituted nearly 75 % of the total (60 nmol m⁻² yr⁻¹). This was about half that measured by Da Silva *et al.* (2006) for the inland Negro River basin (115 nmol m⁻² yr⁻¹). This observation, coupled to comparable fluxes for the South and equatorial Atlantic (18-36 nmol m⁻² yr⁻¹; Lamborg *et al.*, 1999), supports the dominant oceanic contribution of rainfall HgT_{UNF} in the vicinity of the reservoir (Table 4). Considering the emissions, despite the uncertainty surrounding figures, there is a strong suggestion that the reservoir represented a source of Hg⁰ to the atmosphere. Hg⁰ volatilization at the AWI was estimated as 90 ± 50 nmol m⁻² yr⁻¹. This was higher than the average value for the Negro River flooded area (around 20 nmol m⁻² yr⁻¹; Da Silva *et al.*, 2006), but comparable to the data for the Atlantic Ocean (around 110 nmol m⁻² yr⁻¹; Mason *et al.*, 2001; Gårdfeldt *et al.*, 2003c) (Table 4). This result, presumably due to the sparse vegetation cover, typical in permanently flooded areas, underscores the role of tropical reservoirs as local but significant and durable sources of atmospheric Hg. The 2003/04 Petit-Saut reservoir AWI depositions and emissions of Hg averaged 60 and 90 nmol m⁻² yr⁻¹ (i.e. 2800 and 4200 g yr⁻¹), respectively. The reservoir / atmosphere mass balance is thrown all the more out of equilibrium when considering the waters expelled from the dam: DGM exportations then reach 4600 g yr⁻¹ to which one may add the subsequent Sinnamary Estuary degassing. Indeed, from the tailrace monitoring data (Muresan *et al.*, in press), average DGM concentrations in dam discharged waters and the annual exported amount were of the order of 300 ± 200 fmol L⁻¹ and 2 ± 1 moles (i.e. 400 ± 200 grams).

6. Concluding remarks

The present study reinforces the hypothesis that artificial reservoirs in tropical regions constitute important sources for atmospheric Hg. The application of transport-reaction models to Hg distributions from the Petit-Saut reservoir made it possible to monitor the atmospheric sources, determine the periods of production and consumption of DGM, GEM and RGM, and probe the reactions that regulate AWI Hg exchanges. They revealed (Fig. 7) that atmospheric Hg inputs to the reservoir represented 14 moles yr⁻¹ (60 nmol m⁻² yr⁻¹) of which 75 and 3 % corresponded to wet and RGM-mediated deposition (i.e. 46 and 2 nmol m⁻² yr⁻¹), respectively. The associated DGM evasion represented 23 moles yr⁻¹ of which 90 and 10 % corresponded to AWI degassing (90 nmol m⁻² yr⁻¹) and dam discharged amount (180 m³ s⁻¹ at 300 ± 200 fmol L⁻¹). DGM, GEM and RGM displayed marked patterns of day-night cycles including oxidation, deposition, reduction and re-emission processes. These features followed the general pattern of diurnal solar radiation variations: the DGM and RGM levels were found to increase with solar radiation (660 and 0.05 fmol Wh⁻¹ m⁻¹) whereas GEM concentrations declined (- 9 fmol Wh⁻¹ m⁻¹). In surface waters, short period (minute to hour time scale) transformations ought also to be carefully considered. Biologically catalyzed reduction / oxidation mechanisms seemed to play a significant role in controlling reducible Hg speciation and therefore Hg⁰ volatilization. The study of such aphotic mechanisms should be useful to constrain the estimated values required in rapid and/or dark condition evasion models.

Air and rain Hg levels, as determined from the Petit-Saut monitoring enabled us to differentiate between oceanic, terrigenous and anthropic sources. With the notable exception of MMHg_{UNF} (affected by the slash and burn human activity), HgT_{UNF} in rain ($16 \pm 12 \text{ pmol L}^{-1}$) mostly originated from the adjacent Atlantic ocean. The average GEM concentrations at the dam station were also comparable to the mean North Atlantic level (12 ± 2 and 11.5 pmol m^{-3}). To monitor changes in atmospheric Hg partition, future works may use stability constants for calculating Hg^{II} speciation in rain and aerosols with respect to photochemical processes and volatile organic acids (e.g. oxalic and acetic ligands).

Acknowledgments

We would like to thank C. Reynouard and V. Horeau for their help in obtaining the air and rain samples. We also acknowledge F. Schaedlich from Tekran Inc. for his technical assistance. This work was supported by the French National Scientific Research Center (CNRS/PEVS, "Mercury in French Guiana" research program), the European Union Feder funds and the French Ministry for the Environment (MEDD). This work also received the financial support of Electricité de France (EDF) through a scholarship grant to one of us (BM) (#F01381/0). Thanks are due to W. Delor and J. Harris who edited the transcript.

References

- Ababneh FA, Scott SL, Al-Reasi HA, Lean DRS. Photochemical reduction and reoxidation of aqueous mercuric chloride in the presence of ferrioxalate and air. *Sci. Total Environ.* 2006; 367: 831-839.
- Amouroux D, Wasserman JC, Tessier E, Donard OFX. Elemental mercury in the atmosphere of a tropical Amazonian Forest (French Guiana). *Environ. Sci. Technol.* 1999; 33: 3044-3048.
- Amyot M, Auclair JC, Poissant L. In situ high temporal resolution analysis of elemental mercury in natural waters. *Anal. Chim. Acta* 2001; 447: 153-159.
- Amyot M, Mierle G, Lean D, McQueen DJ. Effect of solar radiation on the formation of dissolved gaseous mercury in temperate lakes. *Geochim. Cosmochim. Acta* 1997b; 61: 975-987.
- Beucher C, Wong WCP, Richard C, Mailhot G, Bolte M, Cossa D. Dissolved gaseous mercury formation under UV irradiation of unamended tropical waters from French Guyana. *Sci. Total Environ.* 2002; 290: 131-138.
- Bloom NS. Determination of picogram levels of methylmercury by aqueous phase ethylation followed by cryogenic gas chromatography with cold vapour atomic fluorescence detection. *Can. J. Fish. Aqua. Sci.* 1989; 46: 1131-1140.
- Bloom NS, Watras CJ. Observations of methylmercury in precipitation. *Sci. Total Environ.* 1989; 87-88: 199-207.
- Bloom NS, Fitzgerald WF. Determination of volatile mercury species at picogram level by low temperature gas chromatography with cold-vapour atomic fluorescence detection. *Anal. Chim. Acta* 1988; 28: 151-161.
- Cossa D, Averty B, Bretaudeau J, Sénard AS. Spéciation du mercure dissous dans les eaux marines. Méthodes d'analyse en milieu marin. Editions Ifremer, ISBN 2-84433-125-4, 2003, 27 pp.
- Cossa D, Coquery M, Nakhlé K, Claisse D. Dosage du mercure total et du monométhylmercure dans les organismes et les sédiments marins. Méthodes d'analyse en milieu marin. Editions Ifremer, ISBN 2-84433-105-X, 2002, 27pp.
- Da Silva GS, Jardim WF, Fadini PS. Elemental gaseous mercury flux at the water/air interface over the Negro River basin, Amazon, Brazil. *Sci. Total Environ.* 2006; 368: 189-198.
- Da Silva GS. A dinâmica biogeoquímica do mercúrio na bacia do Negro River (AM) e fluxos na interface água/atmosfera. Doctoral Thesis, Chemistry Institute-State University of Campinas, 2004, 328 pp.
- Dumestre JF, Vaquer A, Gosse P, Richard S, Labroue L. Bacterial ecology of a young equatorial hydroelectric reservoir (Petit-Saut, French Guyana). *Hydrobiol.* 1999; 400: 75-83.
- Fadini PS, Jardim WF. Is the Negro River Basin (Amazon) impacted by naturally occurring mercury? *Sci. Total Environ.* 2000a; 275: 71-82.
- Fitzgerald WF, Mason RP, Vandal GM. Atmospheric cycling and air-water exchange of mercury over mid-continental lacustrine regions. *Water Air Soil Pollut.* 1991; 56: 745-768.
- Fostier H, Forti MC, Guimarães JRD, Melfi AJ, Boulet R, Espirito Santo CM, Krug FJ. Mercury fluxes in a natural forested Amazonian catchment (Serra do Navio, Amapá State, Brazil). *Sci. Total Environ.* 2000; 260: 201-211.
- Garcia E, Poulain AJ, Amyot M, Ariya PA. Diel variations in photoinduced oxidation of Hg^0 in freshwater. *Chemosphere* 2005; 59: 977-981.
- Gårdfeldt K, Jonsson M. Is bimolecular reduction of $Hg(II)$ complexes possible in aqueous systems of environmental importance. *J. Phys. Chem.* 2003a; 107, 4478-4482.
- Gårdfeldt K, Munthe J, Stromberg D, Lindqvist O. A kinetic study on the abiotic methylation of divalent mercury in the aqueous phase. *Sci. Total Environ.* 2003b; 304: 127-136.
- Gårdfeldt K, Sommar J, Ferrara R, Ceccarini C, Lanzillotta E, Munthe J, Wängberg I, Lindqvist O, Pirrone N, Sprovieri F, Pesenti E, Strömberg D. Evasion of mercury from coastal and open waters of the Atlantic Ocean and the Mediterranean Sea. *Atmos. Environ.* 2003c; 37: 73-84.
- Guedron S, Grimaldi C, Chauvel C, Spadini L, Grimaldi M. Weathering versus atmospheric contributions to mercury concentrations in French Guiana soils. *App. Geochem.* 2006; 21: 2010-2022.
- Hall BD, Manolopoulos H, Hurley JP, Schauer JJ, St. Louis VL, Kenski D, Graydon J, Babiarz CL, Cleckner LB, Keeler GJ. Methyl and total mercury in precipitation in the Great Lakes region. *Atmos. Environ.* 2005; 39: 7557-7569.
- Hedgecock IM, Pirrone N, Sprovieri F, Pesanti E. Reactive gaseous mercury in the marine boundary layer. Modelling and Experimental evidence of its formation in the Mediterranean region. *Atmos. Environ.* 2003; 37: 21-39.
- Hedgecock IM, Pirrone N. Mercury and photochemistry in the marine boundary layer-modelling studies suggest the in situ production of reactive gas phase mercury. *Atmos. Environ.* 2001; 35: 3055-3062.

Hornbuckle KC, Jeremiason JD, Sweet CW, Eisenreich SJ. Seasonal variations in air-water exchange of polychlorinated biphenyls in Lake superior. *Environ. Sci. Technol.* 1994; 28: 1491-1501.

Huynh F, Charron C, Betoulle JL, Panechou K, Gardel A, Prost MT, Loubry D. Suivi de l'évolution géomorphologique et botanique de l'estuaire du Sinnamary par télédétection. Final report ORSTOM-EDF, 1997, 64pp.

Iverfeldt A, Lindqvist O. Atmospheric oxidation of elemental mercury by ozone in the aqueous phase. *Atmos. Environ.* 1986; 20: 1567-1573.

Lacerda LD, Ribeiro MG, Cordeiro RC, Sofeddine A, Turcq B. Atmospheric mercury deposition over Brazil during the past 30,000 years. *Ciência e Cultura* 1999; 51: 363-371.

Lamborg CH, Rolfhus KR, Fitzgerald WF, Kim G. The atmospheric cycling and air-sea exchange of mercury species in the South and equatorial Atlantic Ocean. *Deep Sea Res.* 1999; 46: 957-977.

Lanzillotta E, Ceccarini C, Ferrara R, Dini F, Frontini FP, Banchetti R. Importance of the biogenic organic matter in photo-formation of dissolved gaseous mercury in a culture of the marine diatom *Chaetoceros* sp. *Sci. Total Environ.* 2004; 318: 211-221.

Laurier FJG, Mason RP, Whalin L, Kato S. Reactive gaseous mercury formation in the North Pacific Ocean's marine boundary layer: A potential role of halogen chemistry. *J. Geophys. Res.* 2003; 108: art. No. 4529.

Lawson NM, Mason RP. Concentration of Mercury, Methylmercury, Cadmium, Lead, Arsenic, and Selenium in the Rain and Stream Water of Two Contrasting Watersheds in Western Maryland. *Water Res.* 2001; 35: 4039-4052.

Leermarkers M, Galetti S, De Galan S, Brion N, Baeyens W. Mercury in the Souther North Sea and Sheldt Estuary. *Mar. Chem.* 2001; 75: 229-248.

Liang L, Horvat M, Bloom NS. An improved speciation method for mercury by GC/CVAFS after aqueous phase ethylation and room temperature precollection. *Talanta* 1994; 41: 371-379.

Lindberg SE, Zhang H, Gustin M, Vette A, Marsik F, Owens J, Casimir A, Ebinghaus R, Fitzgerald C, Kemp J, Kock HH, London J, Majewski M, Poissant L. Increases in mercury emissions from desert soils in response to rainfall and irrigation. *J. Geophys. Res.* 1999; 104: 21879-21888.

Lindberg SE, Stratton WJ. Atmospheric mercury speciation: Concentrations and behavior of reactive gaseous mercury in ambient air. *Environ. Sci. Technol.* 1998; 32: 49-57.

Lu JY, Schroeder WH. Comparison of conventional filtration and a denuder-based methodology for sampling of particulate-phase mercury in ambient air. *Talanta* 1998; 49: 15-24.

Mason RP, Lawson NM, Sheu GR. Mercury in the Atlantic Ocean: factors controlling air-sea exchange of mercury and its distribution in the upper waters. *Deep Sea Res.* 2001; 48: 2829-2853.

Mason RP, Sheu GR. An examination of the methods for the measurements of reactive gaseous mercury in the atmosphere. *Environ. Sci. Technol.* 2001; 35: 1209-1216.

Mason RP, Lawson NM, Lawrence AL, Joy JL, Lee JG, Sheu GR. Mercury in the Chesapeake Bay. *Mar. Chem.* 1999; 65: 77-96.

Mason RP, Lawson NM, Sullivan KA. The concentration, speciation and sources of mercury in Chesapeake Bay precipitation. *Atmos. Environ.* 1997; 31: 3541-3550.

Mason RP, Sullivan KA. Mercury in Lake Michigan. *Environ. Sci. Technol.* 1997; 31: 942-947.

Mason RP, Fitzgerald WF, Morel FMM. The biogeochemical cycling of elemental mercury: anthropogenic influences. *Geochim. Cosmochim. Acta* 1994a; 58: 3191-3198.

"Mercure en Guyane" program. Charlet L, Boudou A, Grimaldi M, Cossa D. Region de Saint Elie et retenue de Petit-Saut. Final report part 1, 2001, 70pp.

Meteo-France: French institute for weather forecast and meteorological research. 2005 database on wind direction and rain events. <http://www.meteofrance.com>.

Muresan B, Cossa D, Richard S, Dominique Y. Mercury Cycling in a Tropical Artificial Reservoir: Monomethylmercury Production and Sources. *Appl. Geochem.*, in press.

Parker JL, Bloom NS. Preservation and storage techniques for low-level aqueous mercury speciation. *Sci. Total Environ.* 2005; 337: 253-63.

Peretyazhko T, Van Capellen P, Meile C, Coquery M, Musso M, Regnier P, Charlet L. Biogeochemistry of major redox elements and mercury in a tropical reservoir lake (Petit-Saut, French Guiana). *Aquat. Geochem.* 2005; 11: 33-35.

Peretyazhko T, Charlet L, Muresan B, Kazimirov V, Cossa D. Formation of dissolved gaseous mercury in a tropical lake (Petit-Saut reservoir, French Guiana). *Sci. Total Environ.* 2006; 364: 260-271.

Poissant L, Pilote M, Beauvais C, Constant P, Zhang HH. A year of continuous measurements of three atmospheric mercury species (GEM, RGM and Hgp) in southern Québec, Canada. *Atmos. Environ.* 2005; 39: 1275-1287.

Richard S. Monitoring of the IDAF (Igac / Debits / AFrique) network stations of Petit-Saut in French Guiana: the sources of emissions. IDAF/SEARCH workshop 3-5 December 2001, Toulouse, France.

Richard S. La mise en eau du barrage de Petit-Saut. Hydrochimie 1 – du fleuve Sinnamary avant la mise en eau, 2 – de la retenue pendant la mise en eau, 3 – du fleuve en aval. Doctoral Thesis, Aix – Marseille University I, 1996, 278 pp.

Schroeder WH, Anlauf KG, Barrie LA, Lu JY, Steffen A, Schneeberger DR, Berg T. Arctic springtime depletion of mercury. *Nature* 1998; 394: 331-333.

Siciliano SD, O'Driscoll NJ, Lean DRS. Microbial reduction and oxidation of mercury in freshwater lakes. *Environ. Sci. Technol.* 2002; 36: 3064-3068.

Sterm F, Langer E. Increase in global atmospheric concentrations of mercury inferred from measurements over the Atlantic Ocean. *Nature* 1992; 355: 434-436.

Tekran Inc. (2001) Model 1130 mercury speciation unit maintenance manual. Tekran.com.

Vandal GM, Mason RP, Fitzgerald F. Cycling of volatile mercury in temperate lakes. *Water Air Soil Pollut.* 1991; 56: 791-803.

Veiga MM, Hinton J, Lilly C. Mercury in the Amazon: A Comprehensive Review with Special Emphasis on Bioaccumulation and Bioindicators. NIMD (National Institute for Minamata Disease) Forum'99, 1999; 19-39.

Wanninkhof R, Ledwell R, Broecker WS. Gas exchange - wind speed relationship measured with sulfur hexafluoride on a lake. *Science* 1985; 227: 1224-1226.

Hg COMPOUND	DEFINITION	UNIT
TGM	Total Gaseous Mercury (TGM = GEM + RGM)	pmol m ⁻³ (≡ 0.2 ng m ⁻³)
GEM	Gaseous Elemental Mercury	/
RGM	Reactive Gaseous Mercury (Composed of HgCl ₂)	fmol m ⁻³ (≡ 0.2 pg m ⁻³)
HgT	Total Mercury (Sum of all Hg species)	pmol L ⁻¹ (≡ 0.2 ng L ⁻¹)
HgR	Reactive Mercury (pH 1, SnCl ₂ reducible Hg fraction)	/
MMHg	Monomethylmercury	/
DGM	Dissolved Gaseous Mercury (Composed of Hg ⁰)	fmol L ⁻¹ (≡ 0.2 pg L ⁻¹)

TABLE CAPTIONS

Tab. 1. Abbreviation and definition table of the principal mercury (Hg) compounds. Units are according to the International System of Units. Conversion to conventional units (e.g., pg m⁻³ and ng L⁻¹) is displayed in parentheses.

SEASON	GEM / air (pmol m ⁻³)	HgT_{UNF} / rain (pmol L ⁻¹)	DGM / AWM water (fmol L ⁻¹)
Dry seasons	10.9 ± 0.9	20 ± 14	480 ± 270
Met seasons	12.8 ± 1.1	10 ± 6	230 ± 130
Annual	12.0 ± 1.4	16 ± 12	350 ± 200

Tab. 2. Seasonal and annual means (\pm standard deviations) of gaseous elemental (GEM), the sum of all species (HgT_{UNF}) and dissolved gaseous (DGM) mercury. Measurements for GEM (n > 10⁵) in air, HgT_{UNF} (n = 84) in rain and DGM (n = 70) in surface waters corresponds to the Matoutou 1-5 (2003/04) sampling campaigns.

Hg EXCHANGES	FLUXES (nmol m ⁻² yr ⁻¹)	AMOUNTS (moles yr ⁻¹)
Total Hg deposition	40 - 200 (~ 80 on average)	9 - 46 (~ 14 on average)
Wet deposition	46 ± 35	11 ± 8
RGM deposition	2.0 ± 1.5	0.5 ± 0.3
DGM dam exportations		2 ± 1
AWI degassing	90 ± 50	21 ± 11

Tab. 3. Mercury fluxes (and corresponding amounts) at the AWI of Petit-Saut reservoir, and downstream dam DGM exportations.

DOMAIN	RAINFALLS (Hg fluxes in nmol m ⁻² yr ⁻¹)	AWI EFFLUX	REFERENCE
Atlantic Ocean	18-36		Lamborg et al., 1999
	/	39	Mason et al., 1994a
	/	118	Gårdfeldt et al., 2003c
	/	110	Mason et al., 2001
Amazon Basin	115		Da Silva et al., 2008
	/	102	Fadini and Jardim, 2000a
	/	91	Fostier et al., 2000
	/	60	Veiga et al., 1999
	/	20	Da Silva, 2004
Petit-Saut	46 ± 35	90 ± 50	this work

Tab. 4. Comparison of reported values of wet Hg deposition and AWI evasion fluxes from Atlantic Ocean and Amazon Basin with measured values in Petit-Saut area.

FIGURE CAPTIONS

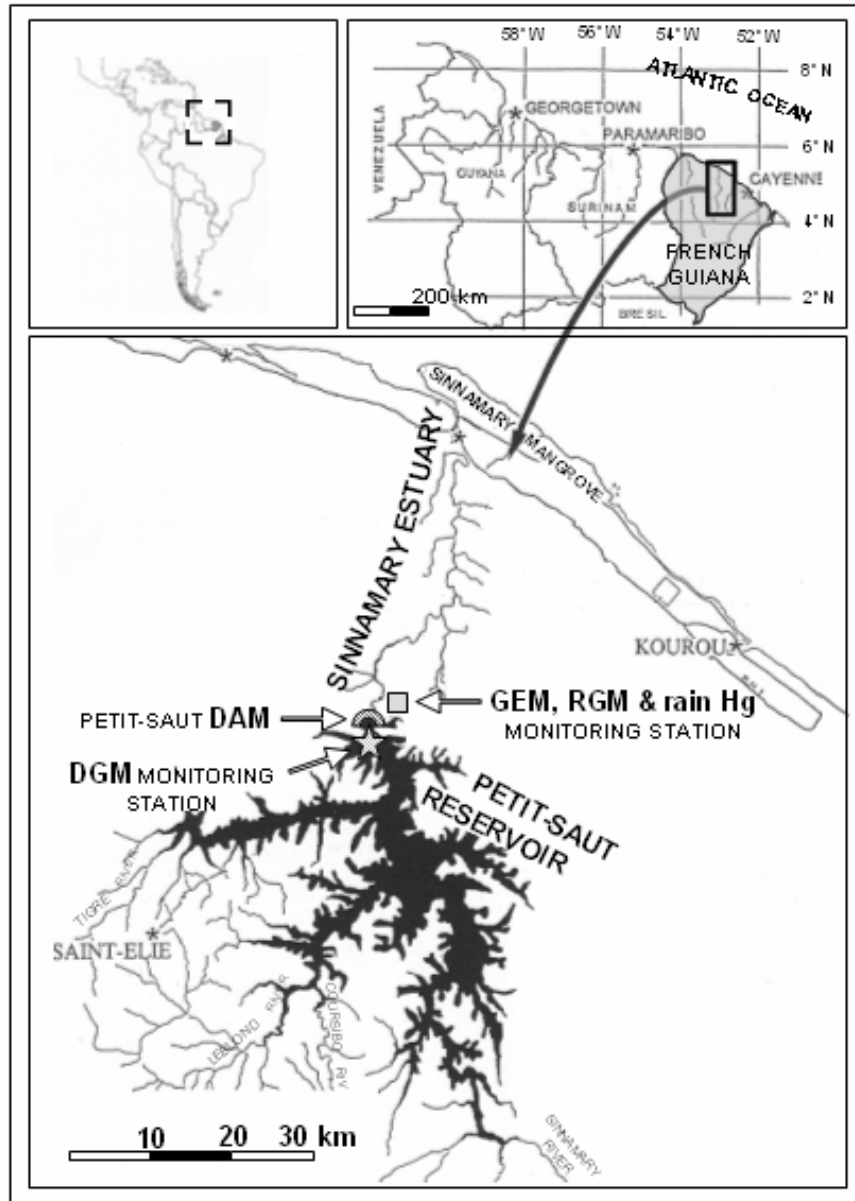


Fig. 1. Location map of the Petit-Saut reservoir / Sinnamary Estuary continuum. Detailed map of the areas where (and dates when) water sampling occurred, including associated geochemical descriptions, is given in Muresan *et al.* (in press).

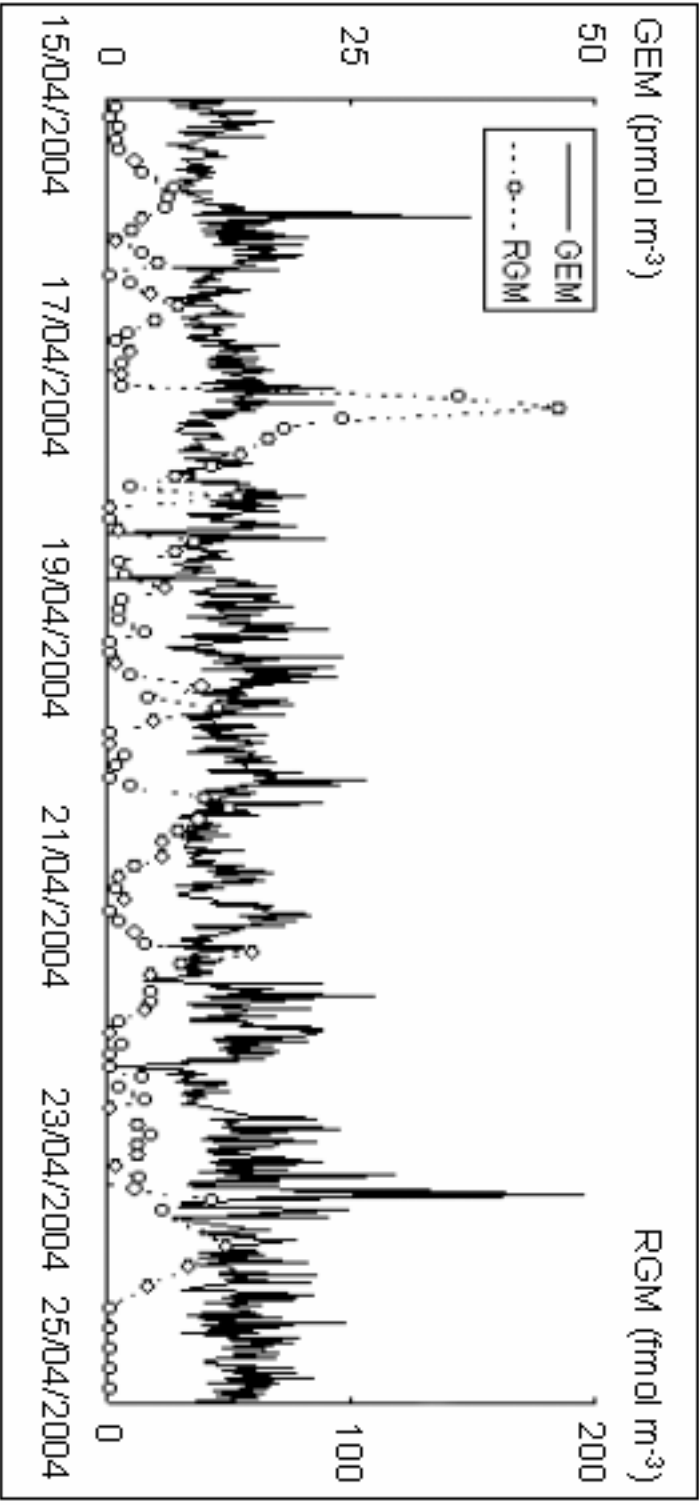


Fig. 2. Monitoring of gaseous elemental (GEM) and reactive gaseous (RGM) mercury concentrations in air. Samples for GEM and RGM were collected on a 5 and 180 min basis at the HYDRECO field laboratory using a Tekran Model 1130 Speciation Unit connected to a Model 2737A vapour analyzer.

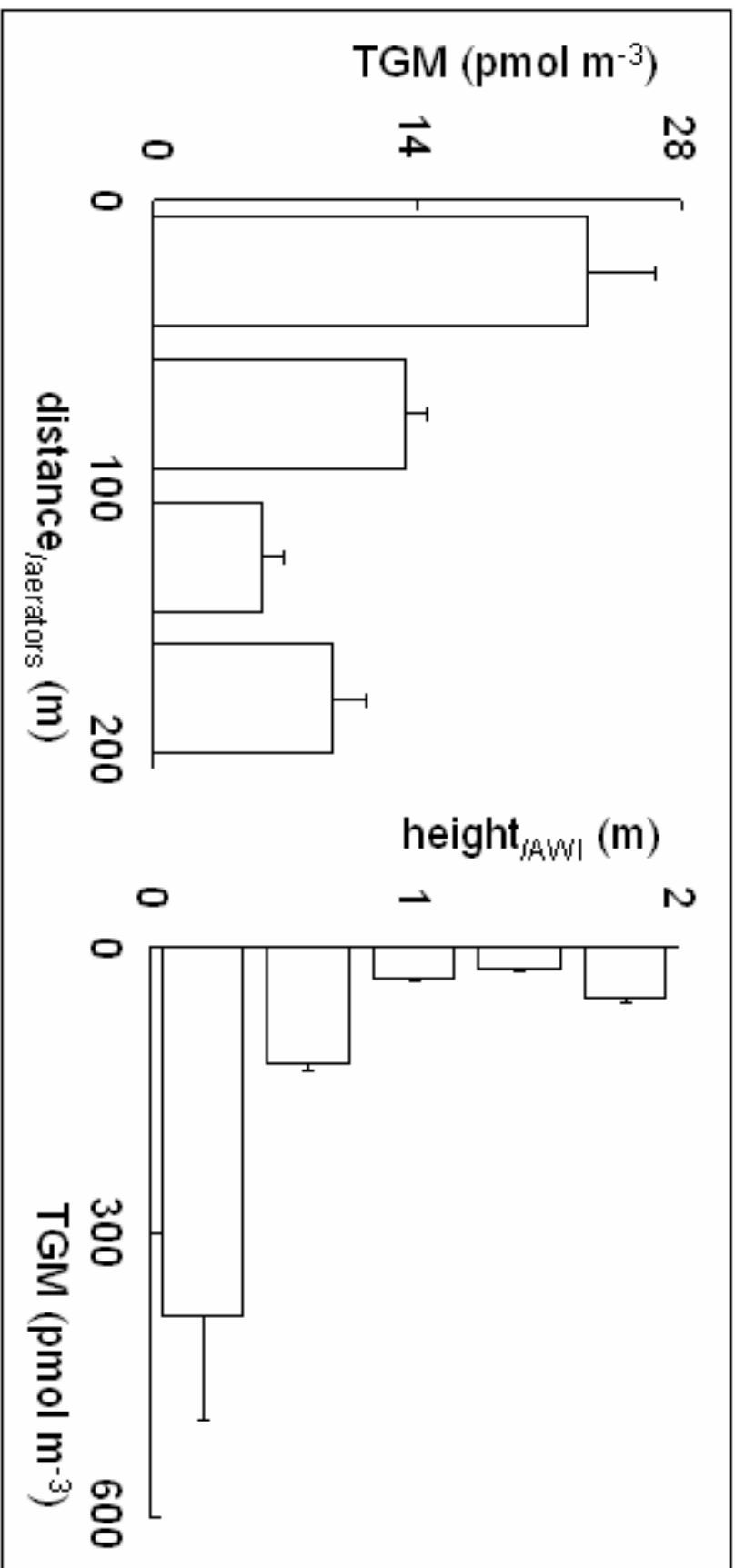


Fig. 3. Transept and height distribution of total gaseous mercury (TGM) in the air-column of the aerators. Error bars represent the mean errors for each sampling. Samples were collected by means of a portable a mercury analyzer RA-915+ (LUMEX) allowing continuous measurements with a detection limit of 10 pmol m⁻³.

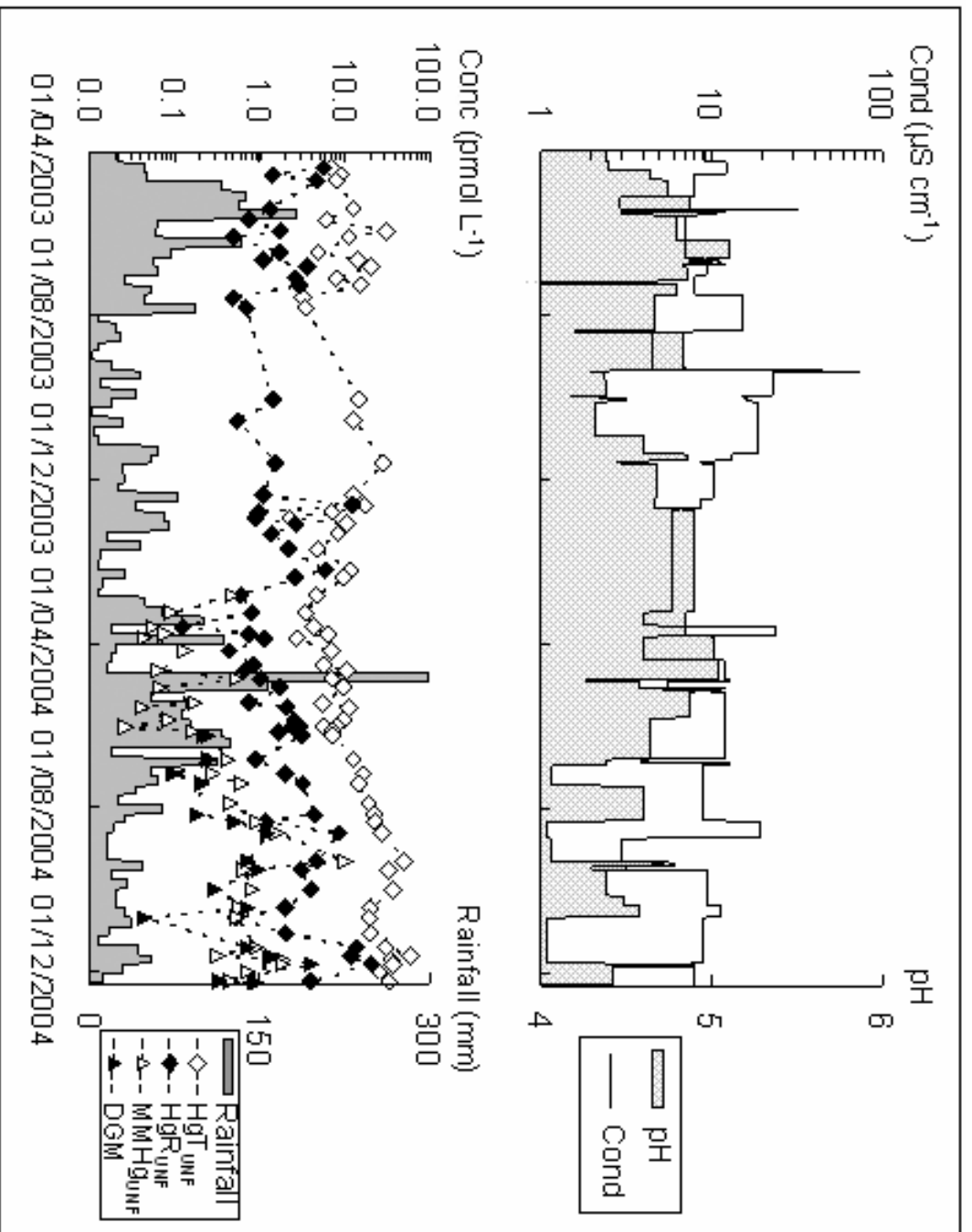


Fig. 4. Monitoring of total (HgT_{UNF}), reactive (HgR_{UNF}), monomethyl (MMHg_{UNF}) and dissolved gaseous (DGM) mercury concentrations in rain. Deposited amount and when achievable pH and conductivity were determined on a weekly basis at the HYDRECO field laboratory.

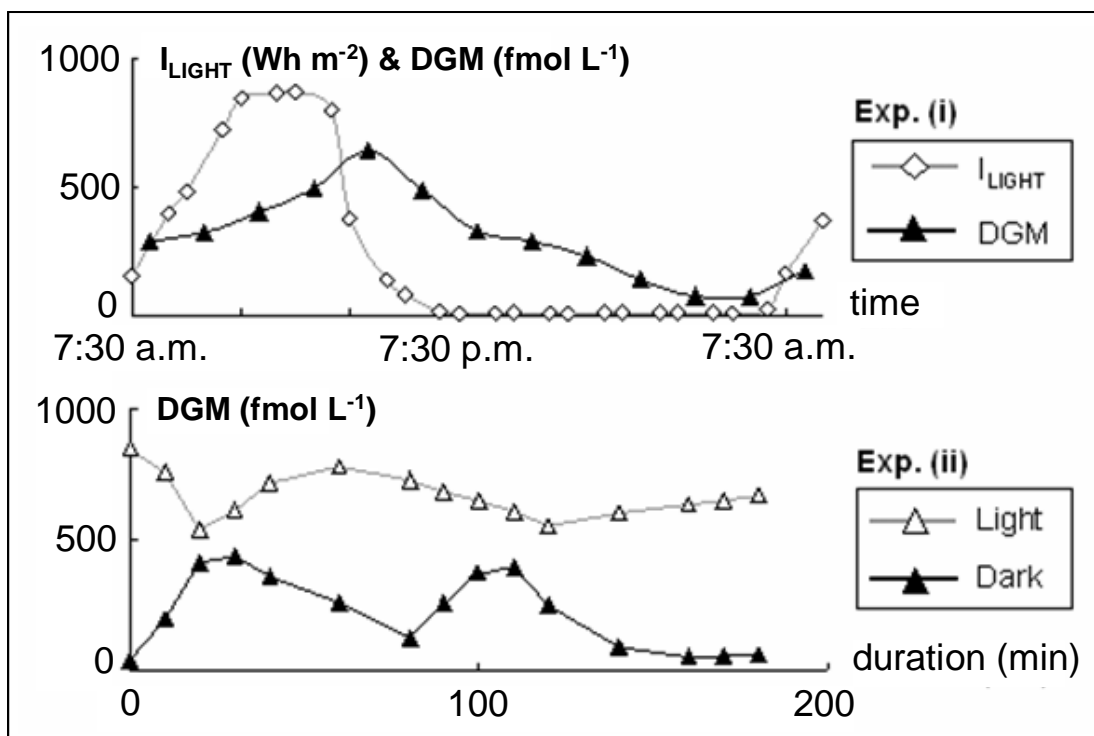


Fig. 5. Exp (i): Diel variations in the intensity of light exposure and dissolved elemental mercury (DGM) concentrations in the Petit-Saut reservoir surface waters. Exp (ii): DGM variations in surface water samples incubated in the dark or under the full spectrum of solar radiation.

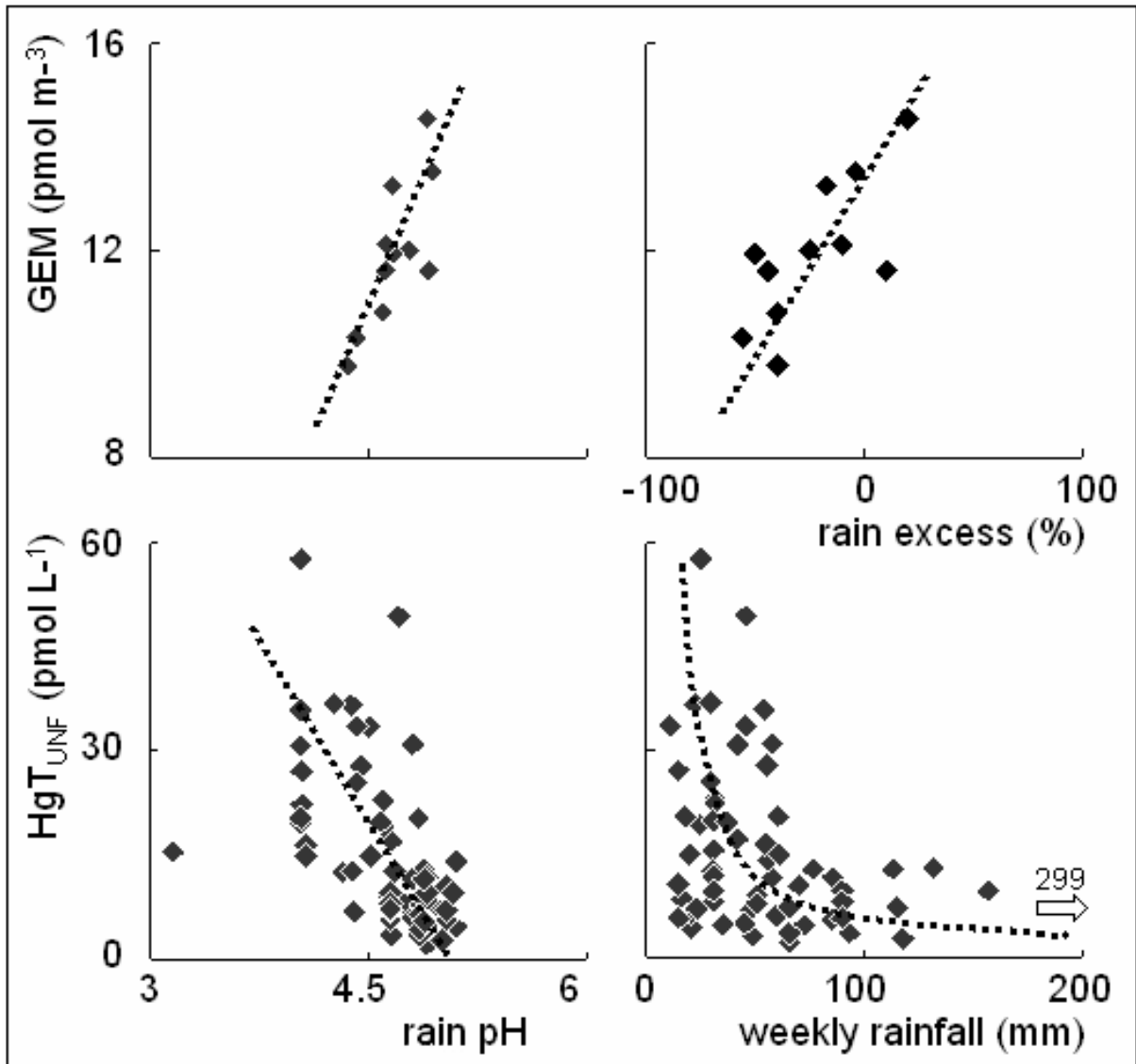


Fig. 6. Upper graphs: monthly GEM concentrations as a function of rain pH and percentage of rain excess. Lower graphs: weekly rain HgT_{UNF} concentrations in relation to rain pH and deposited amounts.

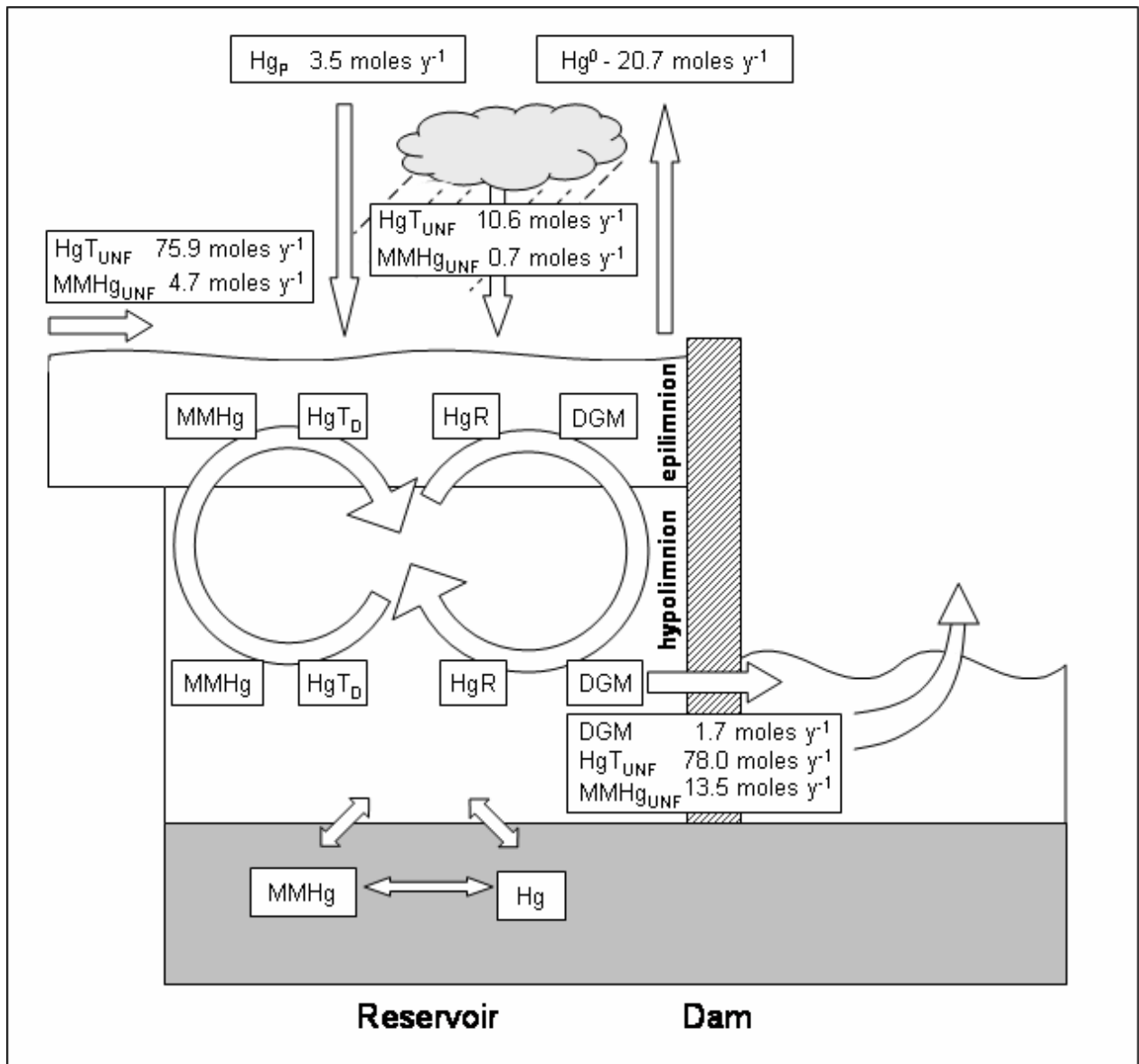


Fig. 7. Mercury budget for the AWI of Petit-Saut reservoir and downstream dam DGM exportations. The whole HgT_{UNF} and $MMHg_{UNF}$ reservoir budget is given in Muresan *et al.* (in press).